SPIE 7842-77
September 29, 2010

Laser damage threshold measurements of anti-reflection microstructures operating in the near UV and mid-infrared

Douglas S. Hobbs*
TelAztec LLC, 15 A Street, Burlington, MA, USA 01803-3404

ABSTRACT

Surface relief textures fabricated in optical components can provide high performance optical functionality such as anti-reflection (AR), wavelength selective high reflection, and polarization filtering. At the Boulder Damage XXXIX symposium in 2007, exceptional pulsed laser damage threshold values were presented for AR microstructures (ARMs) in fused silica measured at five wavelengths ranging from the near ultraviolet (NUV) to the near infrared. For this 2010 symposium, NUV pulsed laser damage measurements were made for ARMs built in fused silica windows in comparison to untreated fused silica windows. NUV threshold values are found to be comparable for both ARMs-treated and untreated windows, however the threshold level was found to be strongly dependent on the material and surface preparation method. Additional infrared wavelength damage testing was conducted for ARMs built in four types of mid-infrared transmitting materials. Infrared laser damage threshold values for the ARMs treated windows, was found to be up to two times higher than untreated and thin-film AR coated windows.

Keywords: Motheye, Antireflection, AR, Microstructures, LIDT, Thin-Film AR Coatings, Laser Damage Threshold

1. INTRODUCTION

The reliability of high power laser systems in medical, industrial, and military applications, is currently limited by the durability of thin-film material coatings needed to produce anti-reflection (AR), high reflection (HR), and filter functions. Thin-film coatings are easily damaged within high power laser systems, and the threshold for coating damage decreases as the demand for higher performance, wider bandwidth, or longer lifetime increases. As a primary example of this performance/reliability tradeoff, developers of missile jamming (infrared countermeasure, or IRCM) systems attempting to scale the power output of fiber lasers and fiber optic beam delivery systems opt for more complex, less stable optical power coupling configurations in order to avoid the use of low damage threshold thin-film AR and HR coatings[1,2]. For ultraviolet (UV) laser system components, thin-film coatings are particularly sensitive to environmental contamination, are prone to material breakdown due to laser absorption, and exhibit short lifetimes that vary considerably depending on the material deposition technique[3,4]. An innovative AR technology based on surface relief microstructures has been shown to have great potential for increasing the reliability and power handling capacity of optical components within high power laser systems[9,19]. AR microstructures (ARMs) etched directly in the surface of relevant materials such as fused silica for UV through NIR laser systems, and infrared transmitting materials such as silicon, sapphire, and diamond, have consistently exhibited damage thresholds that are comparable to or higher than untreated surfaces, a value that equates to a 4 to 5 time increase over any equivalent performance broad-band thin-film AR coated surface. In this work, further measurements of the damage threshold of ARMs treated fused silica windows at 355nm will be given, along with measurements made of ARMs treated materials relevant to mid-IR laser systems.

2. MICROSTRUCTURE BASED ANTI-REFLECTION TECHNOLOGY

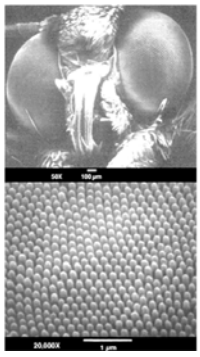

An array of depressions or protrusions that are fabricated in the surface of an optic will function as an effective broadband AR treatment. When such surface relief features are fabricated with dimensions that are small compared to the wavelength of light, they present a gradual change in the refractive index encountered by light propagating through the texture. Reflection losses are reduced to a minimum for broadband light incident over a wide angular range. These graded-index microstructures are commonly known as *Motheye* textures in the literature[5-14] after the eye of nocturnal moths on which the structures were first observed in nature (picture on right). Four distinct types of ARMs, referred to as Motheye, SWS, HYBRID, and RANDOM AR textures are under development. Each type of structure has unique characteristics and optical properties that can be tailored for specific materials and applications. TelAztec has published the performance of ARMs built in numerous materials used in demanding UV, visible, and IR applications[15-23]. A brief outline of two relevant ARMs types is given below;

* dshobbs@telaztec.com; phone 1 781 229-9905; fax 1 781 229-2195; www.telaztec.com

1) MOTHEYE AR Microstructures: Tapered, cone-like structures fabricated in a periodic array in the surface of an optic provide a gradual change of the refractive index for light propagating from air into a bulk optic material. A typical Motheye texture cross section is shown on the left in Fig. 1 where the feature height h and the spacing Λ are indicated.
2) RANDOM AR Microstructures: A simple fabrication process has been developed for AR textures that have a random distribution of sub-wavelength sized surface features. The very small and dense features, as shown in cross section on the right below, provide AR properties that are both extreme and broadband. Advantages of the RANDOM AR texture include the cost driven benefit of eliminating the lithography step necessary for fabricating periodic Motheye structures, and the ability to apply the texture conformal to curved surfaces such as lenses and eyeglasses.

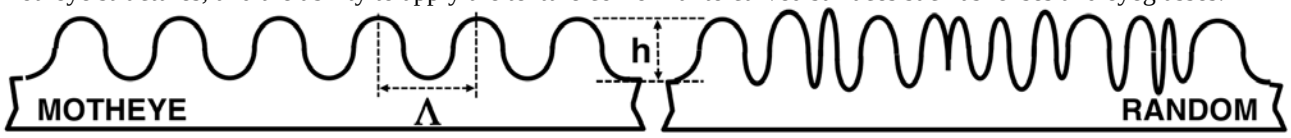

Figure 1: Cross sectional diagrams of typical Motheye (left) and RANDOM (right) ARMs textures.

To achieve high performance AR with surface relief microstructures, optical phenomena such as diffraction and scattering must be avoided. This requires that the surface structures be fabricated with feature spacing (Λ) smaller than the shortest wavelength of operation within the material for a given application. In addition, for the wide bandwidth performance afforded by Motheye and RANDOM ARMs types, the height and cross sectional profile of the surface features must be sufficient to ensure a slow density change. A good rule of thumb is that the height h should be 40% of the longest wavelength within the target application band. Examples of the wide range of materials and applications addressed by ARMs technology are represented by the scanning electron microscope (SEM) images in Figure 2.

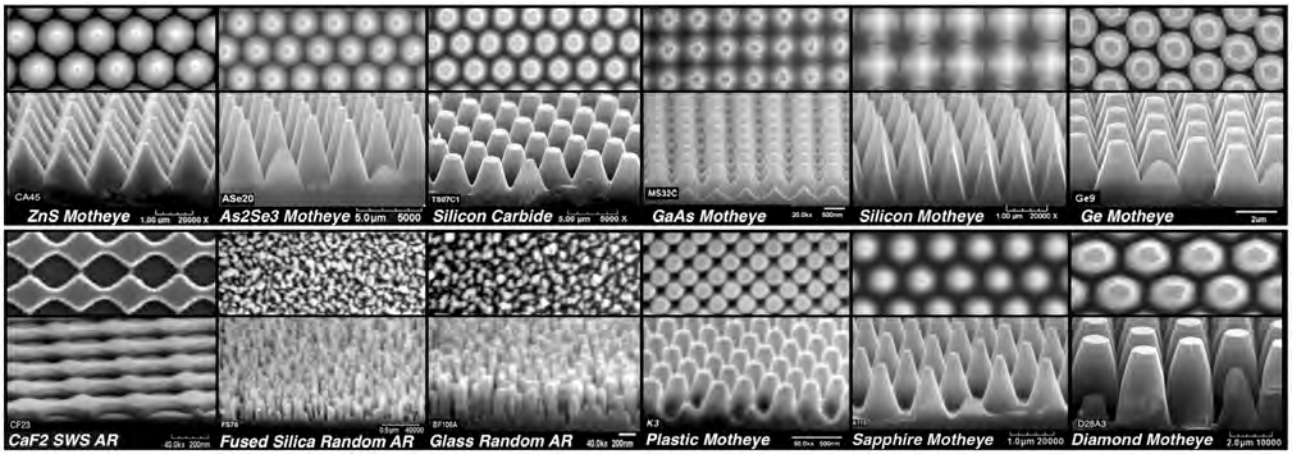

Figure 2: Overhead and Elevation SEM views of ARMs etched in the surface of 12 important optical materials.

A measurement of the typical broad-band performance of ARMs treated fused silica windows is illustrated in Figure 3 (data provided by Omega Optical of Vermont). A normal incidence reflection loss of less than 0.4% (solid black curve) is measured over the 200-800 nanometer (nm) UV-VIS-NIR wavelength range for the RANDOM AR textured surface as compared to the untreated fused silica surface at 3.5% (solid gray line). A magnified overhead view of the RANDOM AR texture in fused silica is shown as an inset to the figure where the typical feature size is in the sub-100nm range and the feature height varies between 200 and 300nm.

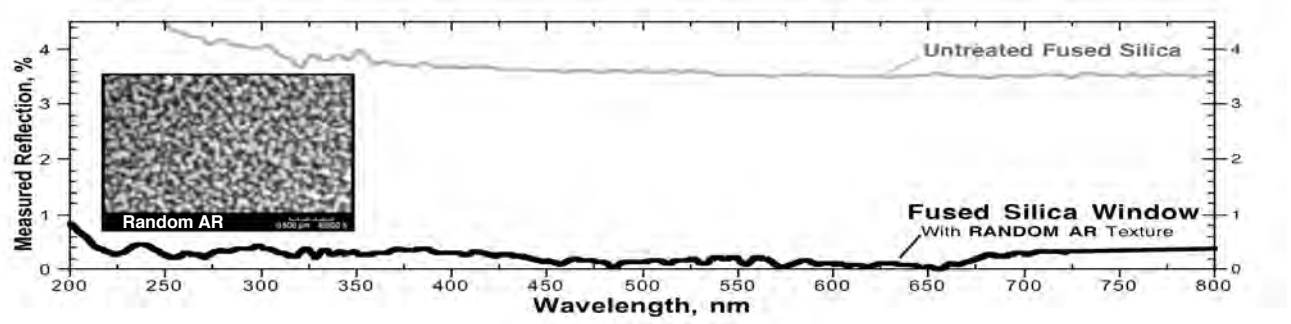

Figure 3: Measured reflection (AOI=10°) from RANDOM AR textured fused silica window (data courtesy Omega Optical).

3. PULSED LASER DAMAGE THRESHOLD MEASUREMENTS

Because both Motheye and RANDOM AR textures provide a gradual change in the refractive index at a material boundary, light can propagate through the boundary without material damage at energy levels that are much higher than that found with thin-film interference AR coatings. In 2007, the pulsed laser induced damage threshold (LiDT) was measured for inexpensive borosilicate glass and fused silica windows containing SWS, Motheye, and Random ARMs textures at multiple wavelengths ranging from the UV through the near infrared[19]. A bar chart summarizing these measurements is shown in Figure 4. At a wavelength of 1064nm, the data shows LiDT values two to five times greater than the highest damage threshold values for thin-film AR coatings often reported in the literature. Reports of the damage threshold of high power infrared laser components with and without thin-film AR coatings consistently show a severe tradeoff between AR performance, bandwidth, and power handling capacity[1,2,23].

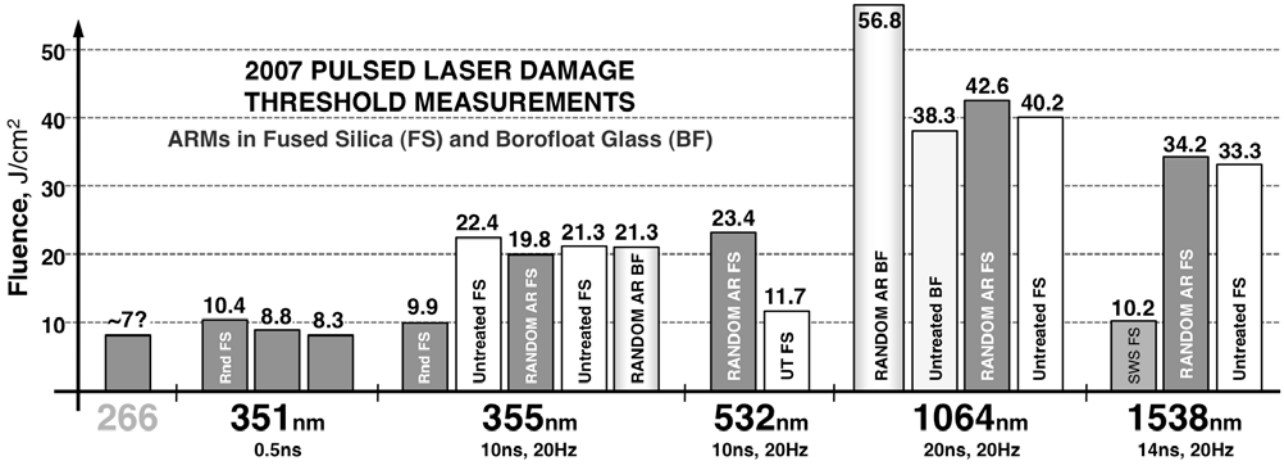

Figure 4: Summary of the pulsed laser damage testing results presented at the 2007 Boulder Damage Symposium.

Standardized pulsed LiDT testing is available as a service from both Quantel USA (formerly Big Sky Laser, Bozeman Montana) and SPICA Technologies (Hollis New Hampshire). The tests conform to International Standards Organization (ISO) 11254, and involve exposing a statistically relevant number of discrete locations (sites) over a sample surface to a calibrated level of laser energy with a specified wavelength, pulse duration, and repetition rate. Referred to as an "S-on-1" test, the typical measurement exposes 100 sites to ten energy levels, 1 energy level per site to obtain a damage frequency verses energy level relationship. The criteria for damage is a permanent surface change observed by visual inspection through a microscope configured for 150X magnification. A linear fit to the damage frequency verses pulse energy data establishes the LiDT.

The LiDT of six materials with and without ARMs textures and thin-film AR coatings was measured at four wavelengths ranging from the long-wave infrared to the NUV. Test results grouped by wavelength are given here;

3.1 LIDT Testing at 9560nm and 10590nm in the long-wave IR

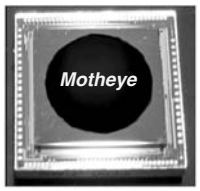

Cadmium Zinc Telluride (CdZnTe) crystals are used as windows and support substrates for infrared imaging sensor arrays based on mercury cadmium telluride HgCdTe diodes. Such sensors require an AR treatment that is broad-band and durable. Motheye ARMs built into the BAE Systems HgCdTe sensor array shown on the right, exhibited extreme optical performance and mechanical reliability. Figure 5 shows scanning electron microscope (SEM) images of two types of ARMs textures built in CdZnTe substrates that are designed for long-wave infrared (LWIR) operation. Typical Motheye ARMs textures, shown on the left in the figure, consist of a honeycomb array of truncated cone structures with a periodic grid spacing of 2.4 micrometer (μm) and a height of 4μm. A binary type, sub-wavelength structure (SWS) ARMs texture, shown on the right in the figure, is simple to fabricate and consists of an array of holes about 1.3μm deep on a 2.4μm grid.

A test of the pulsed laser induced damage threshold of CdZnTe windows incorporating ARMs was conducted at the Air Force Research Laboratory's Laser Hardened Materials Effects Lab (LHMEL) facility at Wright-Patterson Air Force Base in Ohio. Exposures at a wavelength of 9.56 μm compared the damage threshold of Motheye and SWS ARMs in CdZnTe with untreated CdZnTe windows, and a 5-layer thin-film AR coated CdZnTe window consisting of alternating germanium and zinc sulfide materials provided by Raytheon. LWIR transmission measurements for the Motheye (solid gray curve), SWS (thin solid black curve), and thin-film (dashed black curve) AR treated samples, normalized to the untreated substrate transmission, are shown in Figure 6.

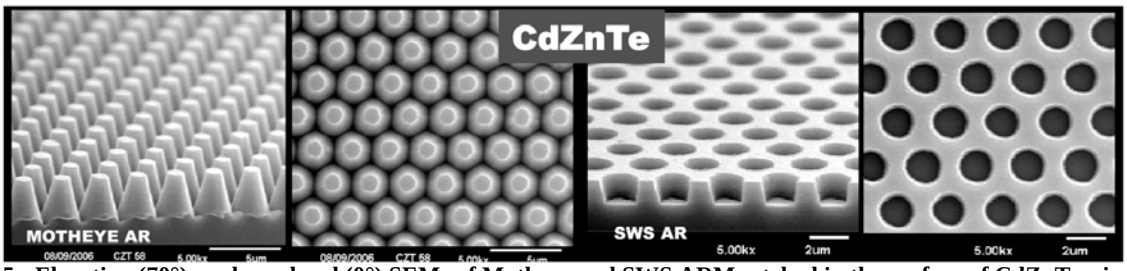

Figure 5: Elevation (70°), and overhead (0°) SEMs of Motheye and SWS ARMs etched in the surface of CdZnTe windows.

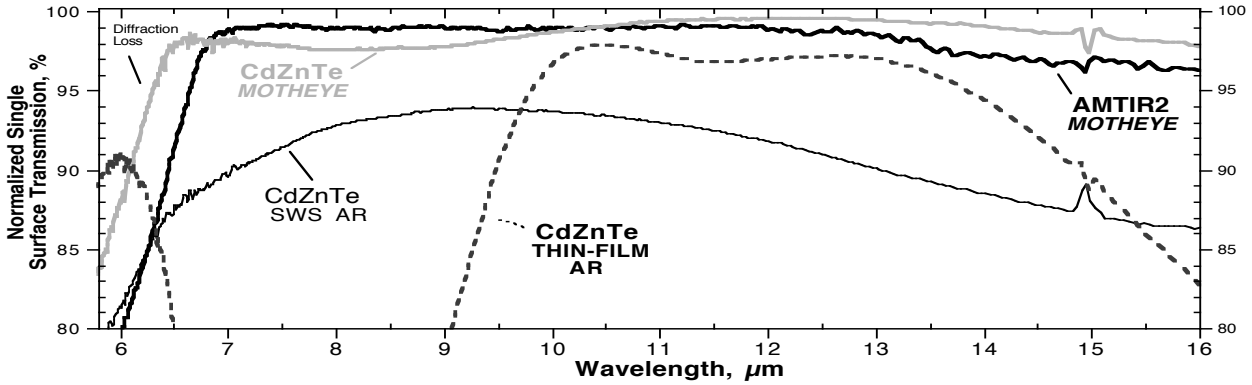

Figure 6: Measured transmission of LWIR light through ARMs treated CdZnTe and AMTIR2 windows, and a multi-layer thin-film AR coated CdZnTe window (all normalized to the untreated window transmission) **prior to LiDT testing.**

Configured for a 180μm ($1/e^2$) spot size, 210 nanosecond (ns) pulse duration, and a 10Hz repetition rate, the LHMEL facility's TEA CO_2 laser exposed 100 locations on each sample, delivering 200 pulses at each location. Ten energy levels were distributed amongst the 100 exposure sites. A plot of the damage frequency verses laser fluence is given in Figure 7 for the four samples tested. The results show damage thresholds for the ARMs treated samples (solid black line/triangles and solid gray line/squares) that are 2-2.5 times greater than the untreated (light grey line/crosses) and thin-film AR coated (open grey squares with dashed line) sample.

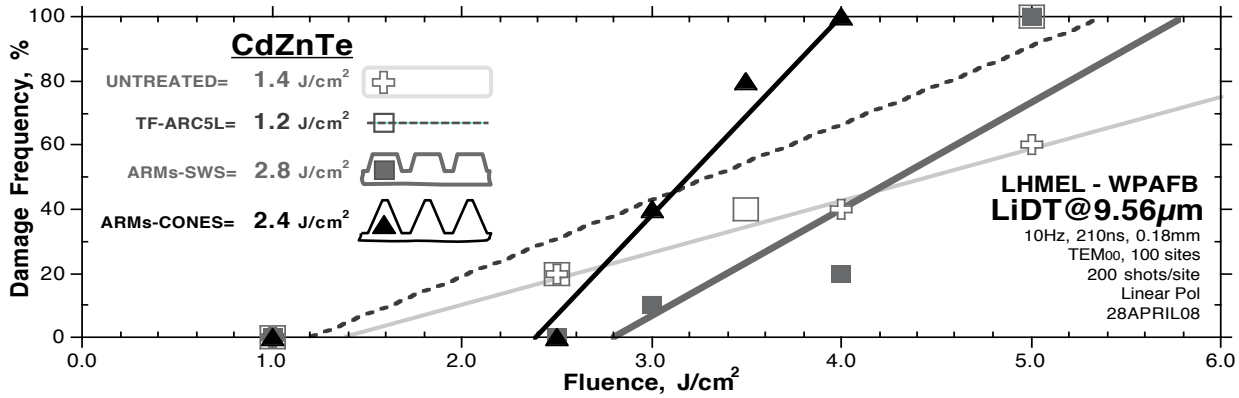

Figure 7: LiDT at 9.56μm of ARMs treated, untreated, and thin-film AR coated CdZnTe windows.

ARMs textures were fabricated in arsenic selenide (As_2Se_3) windows sold commercially as AMTIR2 by Amorphous Materials, Inc. (Garland, TX) as part of a DOE SBIR project aimed at remote sensing applications. SEM images of the Motheye-type ARMs textures fabricated in AMTIR2 are shown in Figure 8. Cone structures 4.8μm high were fabricated in a honeycomb array with a 2.6μm grid spacing. Figure 6 above included the measured LWIR transmission of these Motheye textured AMTIR2 windows (thick solid black line) normalized to the untreated AMTIR2 window transmission. Reflection losses have been reduced to extremely low levels over a wavelength range of from 7 to 16μm, performance that is far superior to any thin-film AR coating designed for the LWIR.

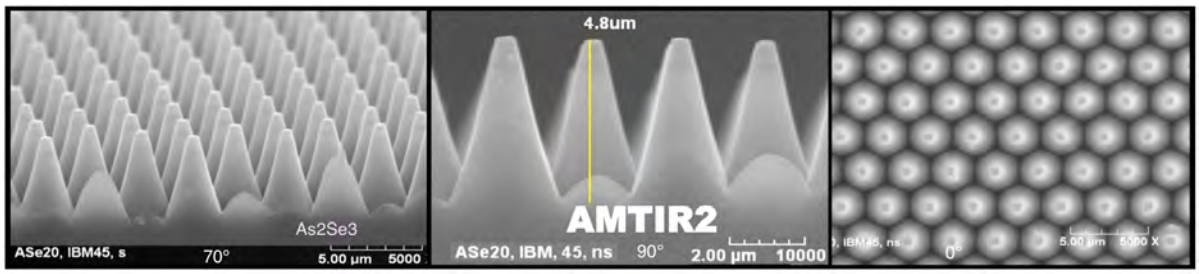

Figure 8: Elevation (70°), profile (90°), and overhead (0°) SEMs of ARMs etched in the surface of an As_2Se_3 window.

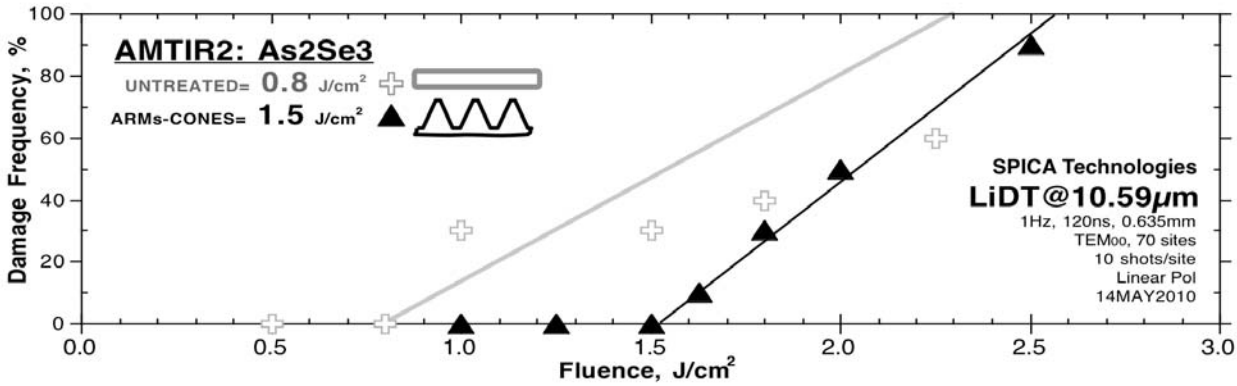

Figure 9: Results of a 10590nm LIDT test of Amorphous Materials AMTIR2 windows with and without Motheye ARMs.

The Motheye textured windows were subjected to standardized LiDT testing at SPICA Technologies using a pulsed CO_2 laser setup operating at a wavelength of 10.59µm. [Because of the toxicity of As_2Se_3 material, SPICA built a custom enclosure over their laser exposure system to exhaust any arsenic vapors that might be liberated during the damage testing.] Seventy sites were exposed on each test sample using a large 635µm spot size, a 120ns pulse duration, and a low repetition rate of just 1Hz. Each site received 10 pulses at one of seven fluence levels. Figure 9 shows the damage frequency as a function of laser fluence for both the ARMs treated (solid black line/triangles) and untreated substrates (solid grey line/open crosses). SPICA found a damage threshold two times higher for the ARMs treated As_2Se_3 windows, as compared to the untreated As_2Se_3 sample (1.5 J/cm^2 vs. 0.8 J/cm^2, respectively).

3.2 LIDT Testing at 2095nm in the mid-infrared

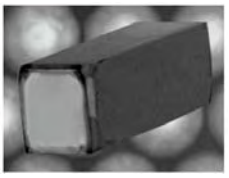

Zinc germanium phosphide ($ZnGeP_2$) is an important mid-IR laser material that can benefit from the potential power handling capacity enhancement provided by ARMs technology. A BAE Systems 6x6x14mm $ZnGeP_2$ crystal used to convert 2µm light into longer wavelength infrared light tunable over the 3.5-4.5µm range, is shown on the right after fabrication of a Motheye-type ARMs texture in the entrance aperture. SEM images showing the 650nm spacing honeycomb array of 700nm high cones that make up the Motheye structure are given in Figure 10. The measured transmission (normalized to the untreated transmission) of an ARMs-treated thin slab cut from the $ZnGeP_2$ crystal is shown in Figure 12 where, as designed, the peak transmission occurs near the pump laser wavelength of 2.1µm.

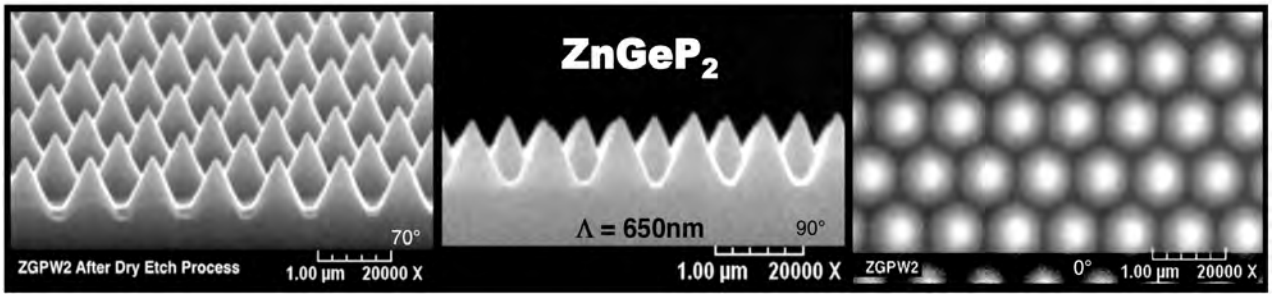

Figure 10: Elevation (70°), profile (90°), and overhead (0°) SEMs of ARMs etched in the surface of a BAE $ZnGeP_2$ crystal.

Initial pulsed LiDT measurements of untreated and ARMs-treated $ZnGeP_2$ crystal slab windows were made using the long pulse duration 2.09µm wavelength laser available at Quantel. Using a 250µm spot size, Quantel exposed up to 80 sites on each sample where each site received 10, 300 microsecond duration pulses, delivered at a rate of 2 pulses each second. Eight fluence levels were distributed amongst the 80 exposure sites over the sample surface. The results, shown in Figure 11, indicate a damage threshold for the ARMs treated $ZnGeP_2$ sample (solid black line/triangles) that is equivalent to the untreated $ZnGeP_2$ window (solid grey line/open crosses) – a value that is likely two times greater than any comparable performance thin-film AR coating.

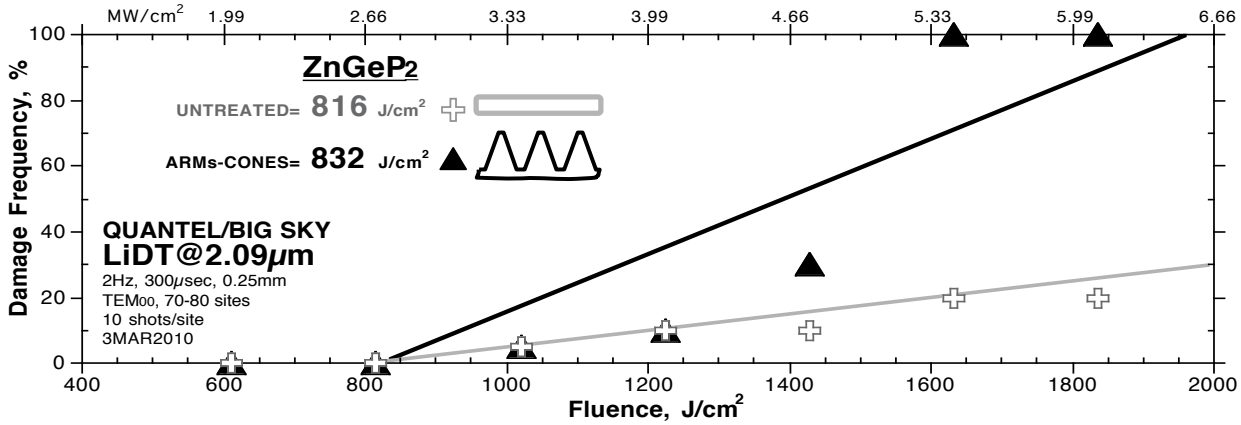

Figure 11: Results of a long pulse duration 2090nm LiDT test of $ZnGeP_2$ windows with and without Motheye ARMs.

The long pulse duration used in this initial test allowed enough time for surface heating effects to produce the observed damage. Figure 13 shows SEM images of comparable size damage sites on the untreated (left) and ARMs-treated (right) $ZnGeP_2$ sample surfaces. Note that the pattern of surface re-modeling contains substantially similar features.

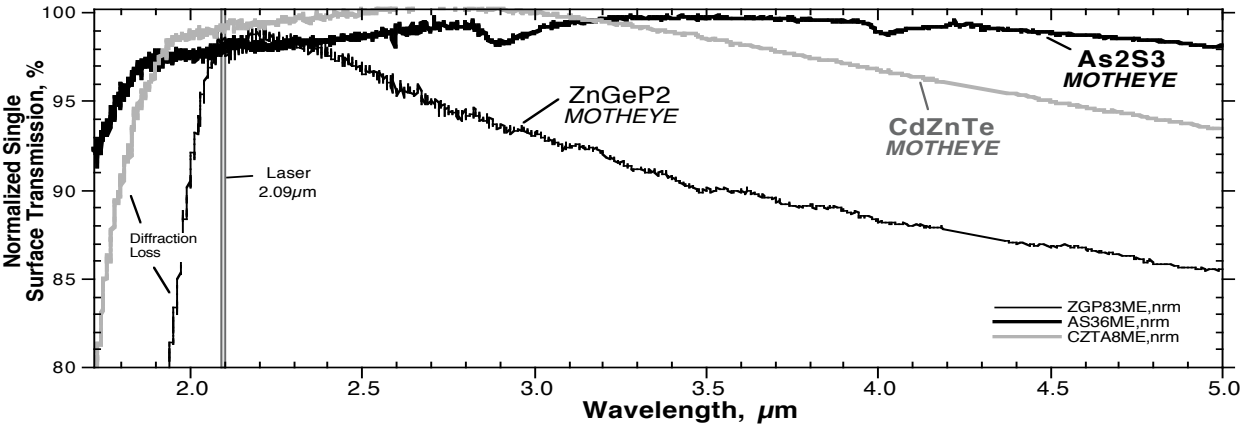

Figure 12: Measured transmission of mid-IR light through ARMs treated $ZnGeP_2$, CdZnTe, and As_2S_3 windows.

Recently a short pulse duration 2.09µm wavelength exposure system became available for LiDT testing at SPICA Technologies. SPICA's system is configured to deliver 80ns duration pulses at a 2Hz repetition rate and a 760µm spot size, 200 pulses each location, 10 energy levels. To exercise the system, Motheye textures designed for mid-IR operation (similar to the 700nm pitch, 1200nm high cone structures shown in Figure 14) were fabricated in CdZnTe substrates, characterized for transmission as shown in Figure 12, and submitted for testing. Figure 15 depicts the results where the damage threshold of the Motheye samples (thick black line/solid triangles, and thin black line/open triangles) is found to be approximately 20% higher than the untreated sample (solid grey line/open crosses). The nature of the damage appears quite different for Motheye-treated surfaces compared to untreated surfaces as depicted in Figure 16. Both the extent of the damaged area and the depth of the damage are smaller in the ARMs-treated surfaces than for the untreated surfaces, a result that would yield lower scattered light loss in an operational system.

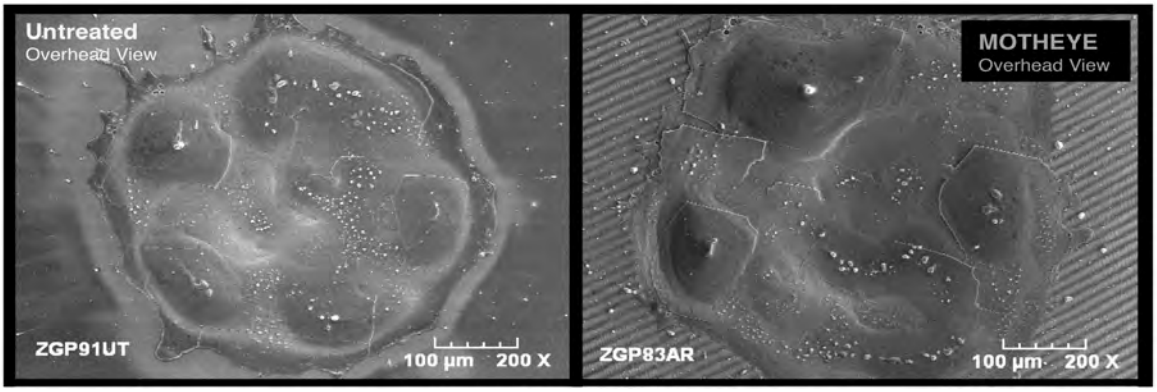

Figure 13: Damage sites in $ZnGeP_2$ without (left) and with (right) Motheye ARMs after long pulse 2090nm LiDT test.

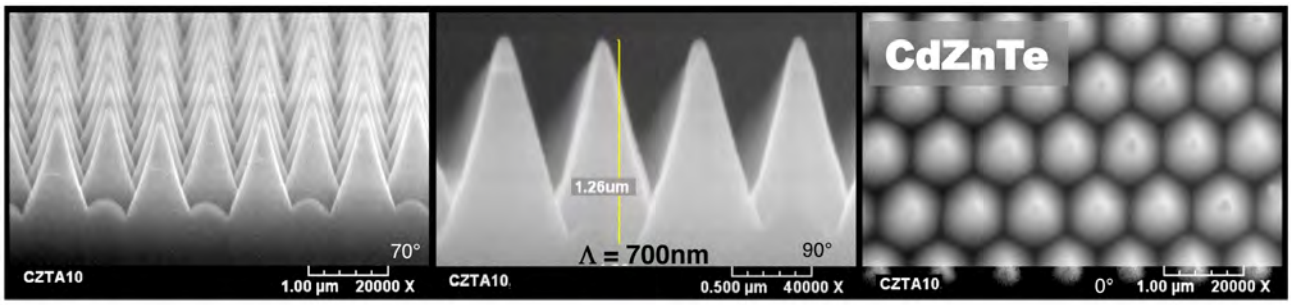

Figure 14: Elevation (70°), profile (90°), and overhead (0°) SEMs of ARMs etched in the surface of a CdZnTe substrate.

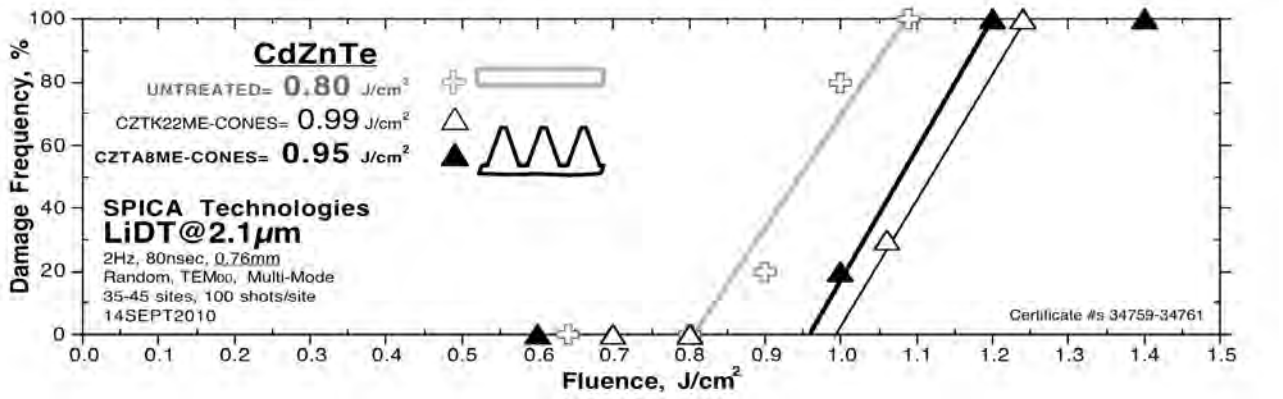

Figure 15: Results of a short pulse duration 2090nm LiDT test of CdZnTe windows with and without Motheye ARMs.

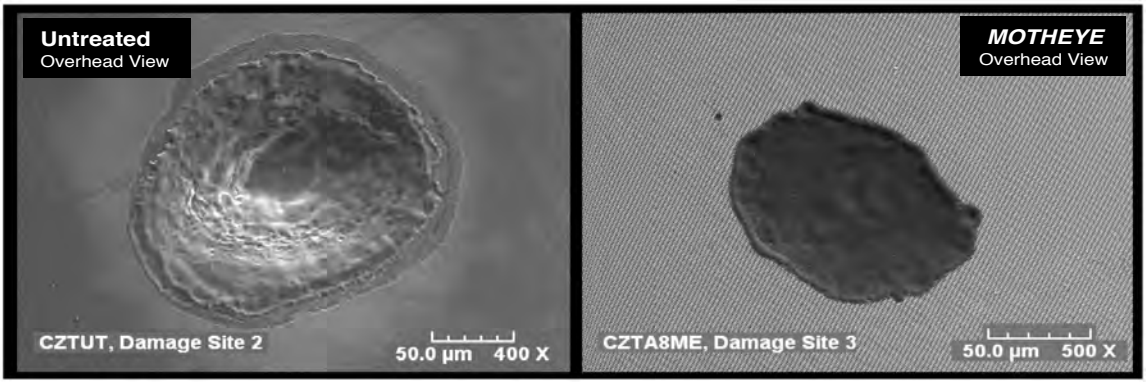

Figure 16: Damage sites in CdZnTe without (left) and with (right) Motheye ARMs after short pulse 2090nm LiDT test.

Fiber optic laser beam delivery systems play a significant role in many military, industrial, and medical high power laser applications. For mid-IR laser sources, optical fiber formed from chalcogenide glass materials such as arsenic tri-sulfide (As_2S_3), have the potential to meet the demanding requirements of next generation missile jamming infrared countermeasure (IRCM) systems. A potential roadblock for the use of As_2S_3 fibers is the power handling limitation imposed by the low damage threshold of conventional thin-film AR coatings needed to suppress harmful reflected light. In addition, the deposition of thin-film AR coatings on the end facets of fiber optic cables is quite difficult and expensive. ARMs technology can provide a cost effective solution to these problems using direct replication of the Motheye texture into the fiber end facets from a master embossing tool. To confirm the potential for improved damage thresholds using ARMs in As_2S_3, Motheye AR textures were designed and fabricated in one surface of As_2S_3 windows supplied by the Naval Research Labs (NRL). Two of these windows are shown on the right together with an As_2S_3 fiber housed in an industry standard connector. Figure 17 shows the pyramidal type structures fabricated where the feature spacing is 740nm and the cone height is about 1500nm. Very high AR performance over a wide mid-IR wavelength range is indicated by the transmission data (thick solid black curve) shown in Figure 12 above. Both ARMs-treated and untreated As_2S_3 windows were submitted to SPICA for LiDT testing at 2.09µm with results as shown in Figure 18. The damage threshold for the Motheye textured surface is found to be 33% higher than the untreated window surface, a result that is likely 2 to 5 times greater than the threshold attainable with a comparable performance thin-film AR coating.

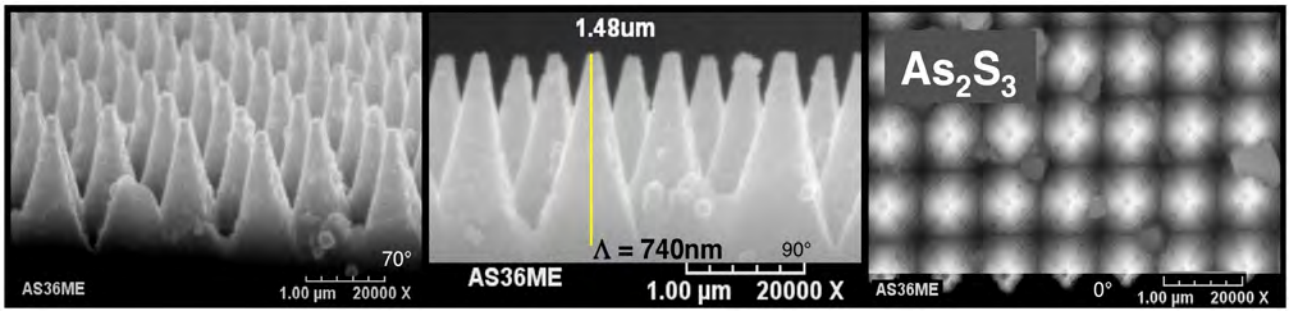

Figure 17: Elevation (70°), profile (90°), and overhead (0°) SEMs of ARMs etched in the surface of an NRL As_2S_3 window.

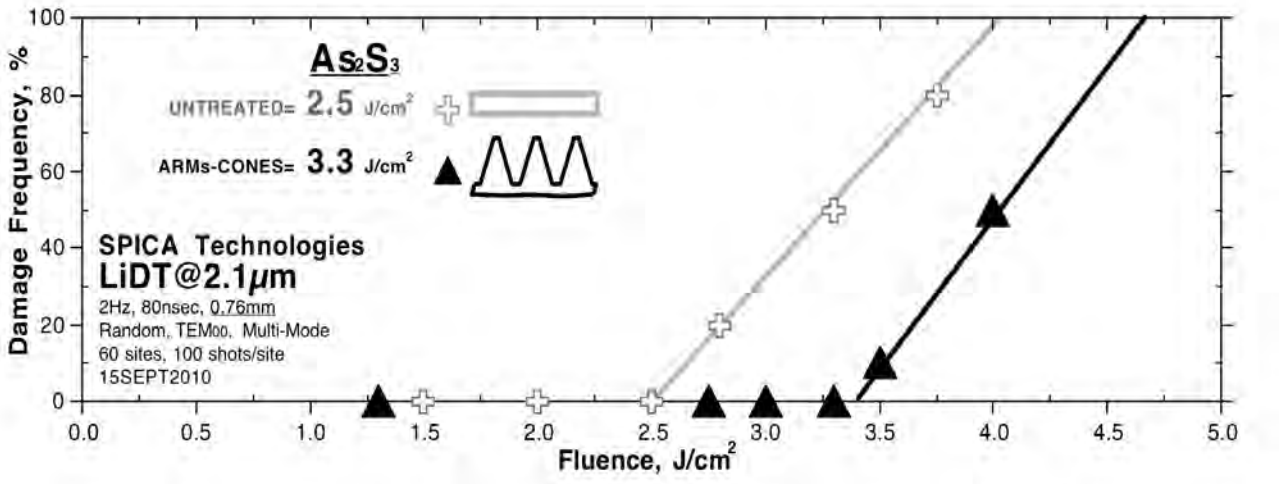

Figure 18: Results of a short pulse duration 2090nm LiDT test of As_2S_3 windows with and without Motheye ARMs.

As with the CdZnTe damage sites produced by the 2.1µm exposures, the nature of the damage produced in As_2S_3 surfaces may indicate a further advantage for ARMs technology. Figure 19 shows elevation view, equivalent area micrographs of damage sites in the surface of untreated (left) and ARMs-treated (right) As_2S_3 windows. A 50-60µm diameter crater over 10µm deep is produced in the untreated As_2S_3 surface, whereas only shallow depth fusing of the microstructures is observed with the ARMs treated surface. Such limited damage should allow the practical and inexpensive re-work of a damaged ARMs treated fiber tip using further embossing.

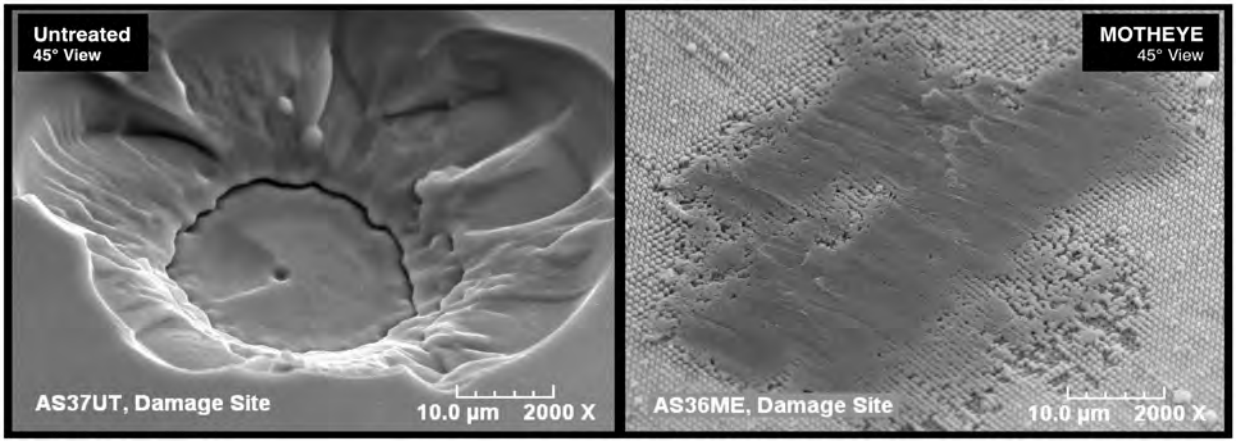

Figure 19: Damage sites in As_2S_3 without (left) and with (right) Motheye ARMs after short pulse 2090nm LiDT test.

3.3 LIDT Testing at 355nm in the near UV

An initial 2007 study of Random ARMs textures produced in fused silica windows showed NUV pulsed laser damage threshold levels as high as 22 J/cm^2 (reference 19 and Figure 4). Many reports in the literature show that the fused silica composition, surface polishing, and post-polish cleaning processes are critical for attaining durability in high power NUV laser systems. Surface preparation methods were investigated in an attempt to further enhance the damage threshold of Random AR-treated fused silica windows.

Three sets of planar test samples were prepared consisting of fused silica from multiple sources and Schott Borofloat 33 glass. Several samples sizes were included. The production of Random AR textures involves an initial cleaning cycle followed by a reactive ion etch process and finishing with a post etch cleaning process. For each test cycle, the reactive ion etch process parameters were adjusted so that the measured reflection from the sample matched the highest performing samples from the 2007 study. In addition, SEM images of witness samples confirmed that the fabricated Random AR texture was consistent with the 2007 samples (Figure 20).

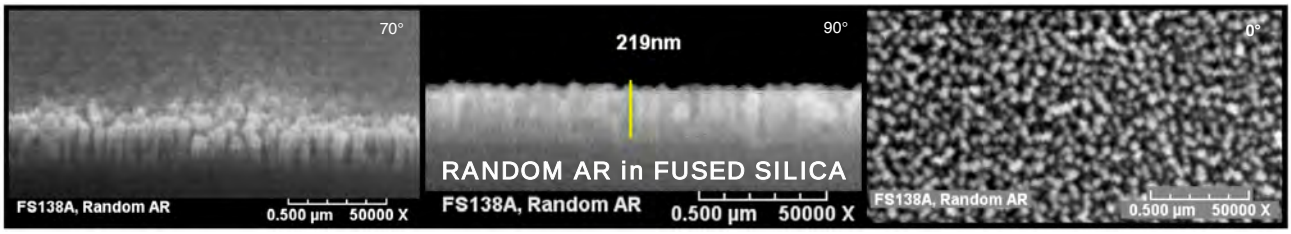

Figure 20: Elevation (70°), profile (90°), and overhead (0°) SEMs of Random ARMs etched in the surface of fused silica.

Figure 21 shows the measured reflection of the first set of test samples. A grating-based spectrometer was employed with a white light source coupled to a fiber-optic reflection probe to deliver light and receive light reflected at near normal incidence. Each sample was optically coupled to a broad-band absorber to eliminate back side reflections. The dashed lines show the reflection from the borofloat glass windows, each 50mm round by 9mm thick. The target reflection for the borofloat glass is also shown from the 2007 work as the dashed grey curve. The reflection from the fused silica samples is given as solid black and grey curves. Note that the solid black curve for sample FS132B is a good performance match to the target sample FS53 from the 2007 study.

It has been reported in the literature that the damage threshold of fused silica optics can be improved using a post-polish wet chemical etch based on hydrofluoric (HF) acid. Consequently, each of the 6 samples prepared for the first cycle of damage testing was immersed in a solution of buffered HF at room temperature for 10 minutes using mild agitation. A modest increase in the visible scattered light level from each sample was observed but not quantified. All samples were then cleaned with a standard acid (H2SO4:H2O2) immersion and solvent rinse followed by a nitrogen blow dry. Random AR textures were then fabricated in both surfaces of two fused silica samples (FS126, FS132) and one

borofloat glass (BF218) sample. A final acid clean was performed on the textured samples prior to submitting the parts for damage testing to remove any surface contaminants introduced during the fabrication or characterization processes. Standard packaging in concave plastic carriers was used to ship the samples to Quantel for damage testing at 355nm.

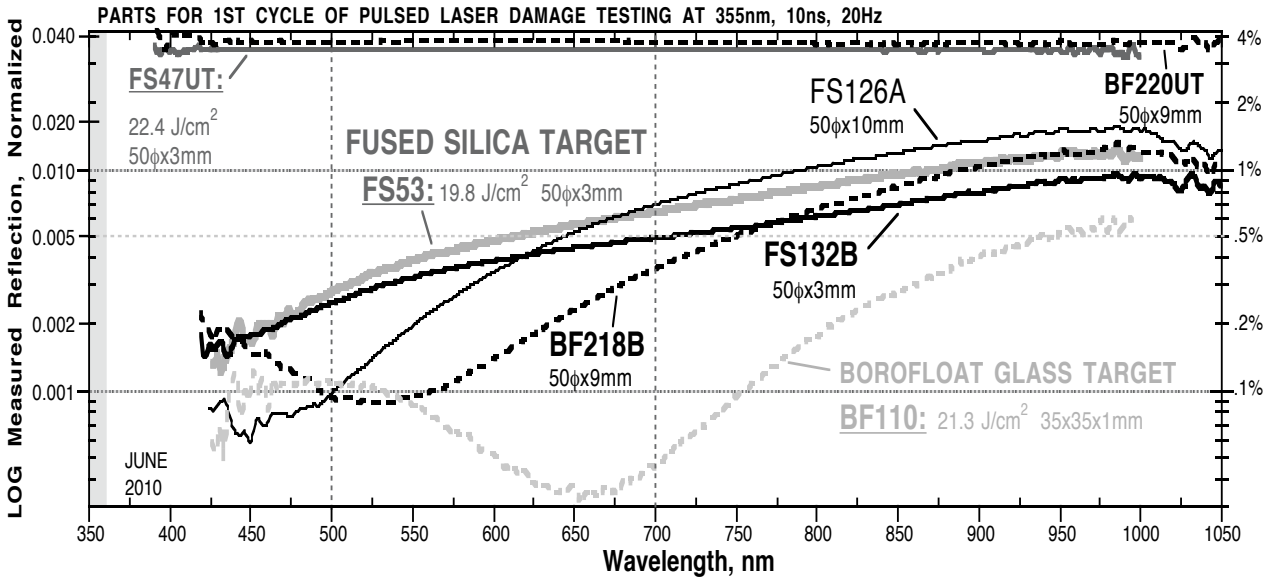

Figure 21: Measured spectral reflectance of Random AR textured samples submitted to the first cycle of NUV LiDT tests.

Quantel exposed more than 100 locations on each window to 10 different fluence levels using a 355nm wavelength, linearly polarized, pulsed laser with a 10ns pulse duration and a 0.35mm spot size (TEM_{00} - $1/e^2$). The pulse repetition rate was 20Hz allowing 200 pulses at each location (10 sec dwell). The criteria for damage was a permanent surface change observed by visual inspection through a microscope configured for Nomarski/Darkfield, 150X magnification. Figure 22 shows a plot of the damage frequency as a function of fluence level where crosses are used for the untreated samples and triangles are used for the Random AR treated samples. Linear fits to the data are depicted as solid and dashed lines and help to illustrate the measured damage threshold. The results indicate damage thresholds far below the 2007 study results. Quantel noted that the scattered light level from these samples that they observe with a red alignment laser was much higher than other samples they have tested. It is likely that the HF post-polish etch process was too aggressive, causing the severe reduction in the measured damage threshold.

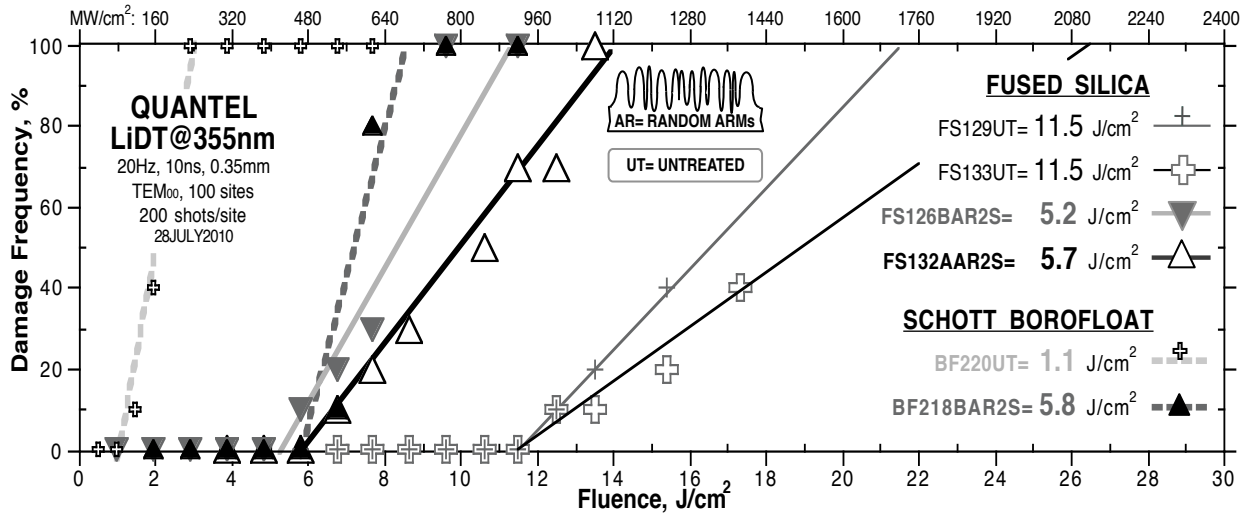

Figure 22: Results of the first cycle of 355nm LiDT testing at Quantel.

Two additional tests were conducted using four samples per cycle. For each cycle the post-polish surface preparation method was modified to produce less scattered light. The results of both rounds of testing were mixed but exhibit levels that remain at less than half those found in the 2007 study. It is clear that surface polish, material composition, surface contaminants, and in particular post polish sub-surface damage mitigation processes are critical for obtaining high damage thresholds for UV optics.

Figure 23 shows a bar graph summarizing the LiDT values measured for ARMs-treated and untreated fused silica and glass windows. An example of the nature of the surface damage found with fused silica substrates as a result of the 355nm laser exposures is shown by the SEM images in Figure 24.

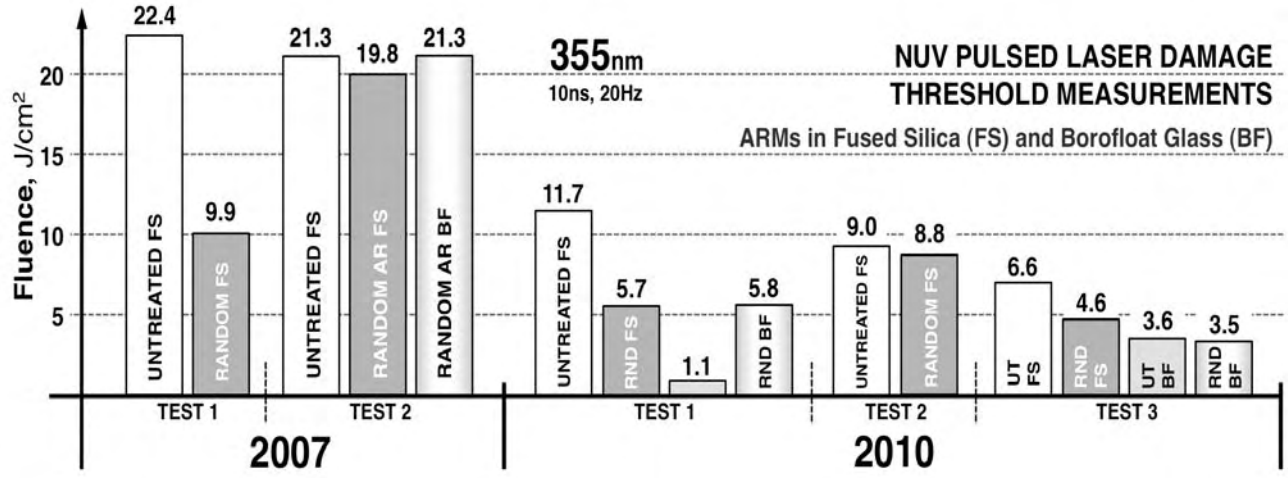

Figure 23: Bar chart summarizing the results of five cycles of 355nm LIDT testing.

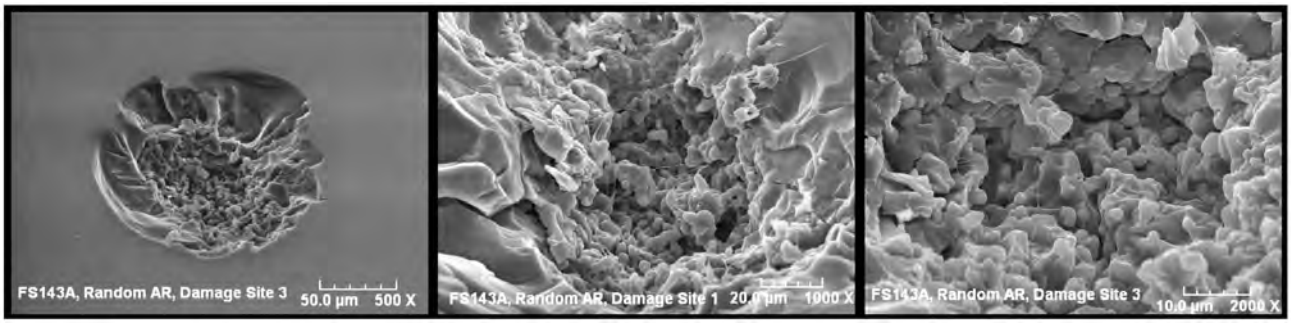

Figure 24: Typical damage site in fused silica after short pulse 355nm LiDT testing. Magnification increases left to right.

4. SUMMARY

AR microstructure technology continues to show great potential for yielding high performance optics with enhanced durability in high power laser systems. In this study, several important mid-infrared transmitting materials fabricated with AR microstructures were shown to have increased transmission over a wide spectral range combined with improved pulsed laser damage thresholds relative to the same materials with no AR treatment. In several cases a factor of 2 higher damage threshold was found relative to conventional thin-film AR coatings with a factor of 5 expected for equivalent AR performance in broad-bandwidth systems such as tunable lasers for medical or environmental monitoring applications. Further studies of the near UV laser damage threshold of Random-type AR microstructures fabricated in fused silica and borosilicate glass, found that surface preparation methods can severely limit the durability of these materials. Additional work is needed to adapt the handling and sub-surface damage mitigation techniques developed by the industry to fully realize the potential of AR microstructure technology in UV laser systems.

5. ACKNOWLEDGEMENTS

The author thanks Jeff Runkel of Quantel USA for providing the certified, NIST traceable LIDT testing in the NUV and at 2.1μm in the mid-infrared. Michael Thomas of SPICA Technologies provided the difficult and hazardous laser damage testing of the chalcogenide materials presented. Leo Gonzales and Shekhar Guha of AFRL's LHMEL facility at WPAFB conducted the pulsed laser damage testing of the ARMs treated CdZnTe windows at 9.56μm. All of the Motheye and Random AR textured samples were fabricated with hard work from Ernest Sabatino, III and Thomas Powers. The SEM analysis was performed by Mr. John Knowles at MicroVision Laboratories, Inc., (978-250-9909).

6. REFERENCES

[1] Berry, P., "Versatile Chromium-Doped Zinc Selenide Infrared Laser Sources", Dissertation- School of Engineering University of Dayton, May (2010).
[2] Wager, Major Torrey J., "Mid-IR Nonlinear Absorption and Damage Study in Ge and GaSb", Air Force Institute of Technology, presentation 22 July (2010).
[3] Zhan, M., et.al., "Stress, absorptance and laser-induced damage threshold properties of 355-nm HR coatings", Applied Physics B, **80**, 1007 (2005).
[4] Gallais, L., et.al., "Laser damage resistance of hafnia thin films deposited by electron beam deposition, reactive low voltage ion plating, and dual ion beam sputtering," Applied Optics, **47**, C107 (2008).
[5] Bernhard, C. G., "Structural and functional adaptation in a visual system", Endeavour, **26**, 79 (1967).
[6] Clapham, P.B., Hutley, M.C., "Reduction of lens reflexion by the 'Moth Eye' principle", Nature, **244**, 281 (1973).
[7] Thornton, B.S., "Limit of moth's eye principle and other impedance-matching corrugations for solar-absorber design." JOSA, **65** (3), 267 (1975).
[8] Wilson, S.J., Hutley, M.C., "The optical properties of 'moth eye' antireflection surfaces", Optica Acta, **29** (7), 993 (1982).
[9] Lowdermilk, W.H. and Milam, D., "Graded-index antireflection surfaces for high-power laser applications", Appl. Physics Letters, **36** (11), 891 (1980).
[10] Cook, L.M., et.al., "Integral Antireflective Surface Production on Optical Glass", Journal of the American Ceramic Society, **65** (9), c152 (1982).
[11] Southwell, W. H., "Pyramid-array surface-relief structures producing antireflection index matching on optical surfaces", JOSA A, **8** (3), 549 (1991).
[12] DeNatale, J. F., et. al., "Fabrication and characterization of diamond moth eye antireflective surfaces on Ge", J. Applied Physics, **71** (3), 1388 (1992).
[13] Harker, A.B., and DeNatale, J.F., "Diamond gradient index 'moth-eye' antireflection surfaces for LWIR windows", Window and Dome Technologies and Materials III, Proc. SPIE, **1760**, 261 (1992).
[14] Raguin, D.H., and Morris, G.M., "Antireflection structured surfaces for the infrared spectral region", Applied Optics, **32** (7), 1154 (1993).
[15] Hobbs, D.S., et. al., "Automated Interference Lithography Systems for Generation of Sub-Micron Feature Size Patterns", Proc. SPIE **3879**, 124 (1999).
[16] MacLeod, B.D., Hobbs, D.S., "Low-Cost Anti-Reflection Technology For Automobile Displays", Journal SID, (2004).
[17] Hobbs, D.S., MacLeod, B.D., "Design, Fabrication and Measured Performance of Anti-Reflecting Surface Textures in Infrared Transmitting Materials", Proc. SPIE **5786**, (2005).
[18] Hobbs, D.S., MacLeod, B.D., "Update on the Development of High Performance Anti-Reflecting Surface Relief Micro-Structures", Proc. SPIE **6545**, 65450Y (2007).
[19] Hobbs, D.S., MacLeod, B.D., "High Laser Damage Threshold Surface Relief Micro-Structures for Anti-Reflection Applications", Proc. SPIE **6720**, 67200L (2007).
[20] MacLeod, B.D., Hobbs, D.S., "Long Life, High Performance Anti-Reflection Treatment for HgCdTe Infrared Focal Plane Arrays", Proc. SPIE **6940**, 69400Y (2008).
[21] Hobbs, D.S., MacLeod, B.D., and Ondercin, R.J., "Initial Erosion Studies of Microstructure-Based Anti-Reflection Treatments in ZnS", 12th DoD Electromagnetic Windows Symposium, (2008).
[22] Hobbs, D.S., et. al., "Performance of HgCdTe IR FPAs Incorporating Microstructure-Based AR Treatments (U)", Military Sensing Symposia, **MSS2009**, (2009).
[23] Hobbs, D.S., "Study of the Environmental and Optical Durability of AR Microstructures in Sapphire, ALON, and Diamond", Proc. SPIE **7302**, 73020J (2009).